

A novel screen-printed microfluidic paper-based electrochemical device for detection of glucose and uric acid in urine

Yong Yao¹ · Chunsun Zhang¹

Published online: 15 September 2016
© Springer Science+Business Media New York 2016

Abstract A novel screen-printed microfluidic paper-based analytical device with all-carbon electrode-enabled electrochemical assay (SP-ACE-EC- μ PAD) has been developed. The fabrication of these devices involved wax screen-printing, which was simple, low-cost and energy-efficient. The working, counter and reference electrodes were screen-printed using carbon ink on the patterned paper devices. Different wax screen-printing processes were examined and optimized, which led to an improved method with a shorter heating time (~ 5 s) and a lower heating temperature (75 °C). Different printing screens were examined, with a 300-mesh polyester screen yielding the highest quality wax screen-prints. The carbon electrodes were screen-printed on the μ PADs and then examined using cyclic voltammetry. The analytical performance of the SP-ACE-EC- μ PADs for the detection of glucose and uric acid in standard solutions was investigated. The results were reproducible, with a linear relationship [$R^2 = 0.9987$ (glucose) or 0.9997 (uric acid)] within the concentration range of interest, and with detection limits as low as 0.35 mM (glucose) and 0.08 mM (uric acid). To determine the clinical utility of the μ PADs, chronoamperometry was used to analyze glucose and uric acid in real urine samples using the standard addition method. Our devices were able to detect the analytes of interest in complex real-world biological samples, and have the potential for use in a wide variety of applications.

Electronic supplementary material The online version of this article (doi:10.1007/s10544-016-0115-6) contains supplementary material, which is available to authorized users.

✉ Chunsun Zhang
zhangcs@sncu.edu.cn; zhangcs_sncu@126.com

¹ MOE Key Laboratory of Laser Life Science & Institute of Laser Life Science, College of Biophotonics, South China Normal University, Guangzhou 510631, China

Keywords Screen-printed carbon electrodes · Wax-screen-printed patterned papers · Electrochemical detection · Glucose · Uric acid · Urine analysis

1 Introduction

The development of simple, rapid, and low-cost analytical devices is of considerable interest for biomedical and analytical chemistry because of the strong demand for many applications, including environmental monitoring, early screening of diseases and food quality control, especially in remote and rural areas in developing countries (Tan et al. 2010; Xiang and Lu 2011; Lawrence et al. 2014; Wang et al. 2014; Dossi et al. 2013). Current chemical and biochemical assays are time-consuming, require expensive instruments and high workloads, and consume large amounts of samples and reagents. To reduce the time, cost, and labor, lab-on-a-chip (LOC) devices or micro total analysis systems (μ TAS) have been developed to minimize the scale of traditional laboratory tests (Santhiago and Kubota 2013). However, the fabrication processes required for silicon, glass or polymer-based LOC devices are often complicated, as demonstrated by the need for mechanical components, such as micropumps or microvalves, to control the flow of the solution in the microfluidic device (Zhang et al. 2007). In 2007, Whitesides and co-workers proposed the use of patterned paper as a platform for microfluidic bioassays (Martinez et al. 2007). Since then, the microfluidic paper-based analytical devices (μ PADs) have received extensive attention because they are cheap, simple, portable, and disposable, only require small amounts of reagents and samples, and show potential for mass production (Martinez et al. 2010).

To date, many detection methods have been developed for the qualitative and quantitative analyses of analytes using μ PADs (Yetisen et al. 2013), including colorimetric

(Rattanarat et al. 2014), fluorescence (Thom et al. 2014), electrochemical (EC) (Carvalho et al. 2010; Määttä et al. 2013; Shiroma et al. 2012; Tan et al. 2010, 2012; Lawrence et al. 2014), chemiluminescent (Wang et al. 2012), and electrochemiluminescent methods (Delaney et al. 2011; Main et al. 2013). In addition to the advantages outlined previously, some of these detection methods also allow for the development of precise and sensitive analytical devices. EC detection is particularly suitable for integration within μ PADs because it enables the rapid quantification of analytes with high sensitivity and specificity, and does not require a dark environment. Additionally, the fabrication of μ PADs that incorporate EC detection is compatible with mature micromachining methods. To date, there are very few examples of EC containing μ PADs with electrodes that have been completely fabricated using inexpensive carbon ink. The fabrication of the electrodes often consists of two layers; one serves as both the reference electrode and conductive pads, and the other as the counter and working electrodes. As a result, the formation of these electrodes is complicated and costly. Additionally, an extra adhesive layer is often required for the assembly of paper-based devices on top of these three-electrode substrates, which adds to the complexity of the system.

Several methods for the fabrication of paper-based EC devices have been reported, including photolithography (Dungchai et al. 2009; Nie et al. 2010b), inkjet printing (Määttä et al. 2011, 2013, 2014), wax printing (Nie et al. 2010a; Rattanarat et al. 2014; Shiroma et al. 2012), wax pencil-based patterning (Liu and Crooks 2012), wax dipping (Noiphung et al. 2013), paper cutting (Lawrence et al. 2014; Kong et al. 2014; Tan et al. 2010, 2012), and lacquer spraying (Nurak et al. 2013). Each different fabrication method has advantages and limitations that have been described in detail in previous reports (Lu et al. 2009; Songjaroen et al. 2011; Nurak et al. 2013).

Two significant obstacles that must be overcome to allow the fabrication of μ PADs for applications in developing countries are the cost of the fabrication instrument and the resolution of the fabrication method. Additionally, environmental concerns must be addressed to ensure that fabrication methods and materials do not pose disposal hazards. Taking these factors into account, the wax screen-printing method shows great promise for the fabrication of μ PADs. Screen-printing provides a convenient way to transfer a printable material onto a paper substrate with desired images or shapes. Wax screen-printing uses solid wax, which is often inexpensive and non-toxic, and the screen-printing process only requires a hot plate for patterning the wax into paper. In 2011, Henry and co-workers reported the use of wax screen-printing for the fabrication of μ PADs (Dungchai et al. 2011). However, high heating temperatures (100 °C) and long heating times (60 s) were required. Using a similar process, Yu's group developed paper-based microfluidic devices for chemiluminescent

sensing, which required heating at 130 °C for 150 s to ensure penetration of the wax into the paper (Wang et al. 2012, 2013). Wax screen-printing that requires high temperatures and long times is not compatible from an environmentally friendly and energy efficiency standpoint, especially for mass production. To the best of our knowledge, there are no reports that attempt to make the conventional wax screen-printing fabrication of paper-based EC devices more environmentally friendly and energy efficient.

In this study, an improved wax screen-printing approach was explored for the fabrication of paper-based cells for EC detection. By using carbon ink as a fabrication material, the working, counter and reference electrodes were simultaneously screen-printed on patterned paper. This was a simple, inexpensive, and environmentally friendly approach to fabricate screen-printed μ PAD with an all-carbon electrode-enabled electrochemical assay (SP-ACE-EC- μ PAD). Compared with conventional paper-based wax-screen-printing, our improved fabrication method required a significantly shorter wax-melting time and a lower heating temperature to ensure the penetration of the wax into the paper. The two main advantages of using a short melting time for wax-printed patterns are as follows: (1) the short melting time can lead to a small energy consumption at a certain heating temperature, and the resulting fabrication process may be compatible with portable microfluidic thermal devices for applications in the field environment (Jiang et al. 2014); and (2) under the conditions where the printing wax is at sufficient quantity and the melting temperature is adequate, the relatively short melting time may be beneficial to the generation of the desired hydrophobic barriers and hydrophilic chambers (or channels) (Liu et al. 2015). Similar to conventional EC systems, the screen-printed three-carbon-electrode system exhibited a good EC characterization (i.e., the EC reaction on carbon electrodes was a diffusion-controlled, reversible process). The analytical performance of the SP-ACE-EC- μ PAD was evaluated and then used to determine the concentrations of glucose and uric acid in real urine samples.

2 Experimental

2.1 Materials and reagents

Whatman #1 chromatography paper (200 mm \times 200 mm, pure cellulose paper) with relatively uniform thickness and wicking properties (Martinez et al. 2010) was purchased from GE Healthcare Worldwide (Shanghai, China) and used with further adjustment of size. Carbon ink (model number CNB-7, <60 Ω /square) and silver/silver chloride ink (model number CNC-01, 100–350 m Ω /square) were purchased from Xuzhou Bohui New Materials Technology Co., Ltd. (Xuzhou, China). Crayons (Detong Co., Ltd., Guangzhou, China) and a smooth

metal utensil were obtained from a local department store. Potassium chloride, potassium ferricyanide (III), α -D-glucose and glucose oxidase (100 U/mg, *Aspergillus niger*) were purchased from Sigma-Aldrich (St. Louis, MO, USA). Uric acid, uricase (10 U/mg) and ferrocene carboxylic acid were purchased from J&K Chemical Ltd. (Beijing, China). Phosphate-buffered solution (PBS; 20 \times) and bovine serum albumin (BSA) were obtained from Sangon Biotech (Shanghai) Co., Ltd. (Shanghai, China). Sodium hydroxide was purchased from the Guangzhou Chemical Reagent Factory (Guangzhou, China). Carmine food dye was obtained from Chengdu Xiya Chemical Technology Co., Ltd. (Chengdu, China). The clinical human urine samples were provided by Guangzhou First People's Hospital. All chemicals were used as received without further purification.

2.2 Apparatus

EC measurements were recorded using a handheld bipotentiostat device (CHI 1242B, Shanghai CH Instruments, China). A water-purification system (≥ 18 M Ω , Elga Purelab@Option-R15, London, UK) was used to obtain deionized (DI) water. The numerical control ultrasonic cleaner (KQ-100DA) was purchased from Kunshan Ultrasonic Instruments Co., Ltd. (Kunshan, China). A microcomputer temperature controlled heating board (YH-946B) was obtained from Guangzhou Yihua Electronic Equipments Co., Ltd. (Guangzhou, China). The screens were custom-made by the Lianchang Printing Equipment Shop (Guangzhou, China).

2.3 Fabrication of the SP-ACE-EC- μ PAD

The SP-ACE-EC- μ PAD was prepared on the filter paper, as shown schematically in Fig. 1. The patterns for the screens that defined the EC cells and electrodes (paper-cell screen and electrode screen) were designed using Adobe Illustrator software (Adobe Systems Inc.), which were used to produce the paper-cell screen (200 or 300 mesh nylon, 200 or 300 mesh polyester) and the electrode screen (300 mesh polyester). The white areas on the screen allowed solid wax or carbon ink to form hydrophobic areas or the electrodes on the paper substrate, respectively. The green areas yielded hydrophilic cells (cells of \varnothing 11 mm were used to evaluate the fabrication methods and cells of \varnothing 15 mm were used for the EC experiments).

The paper (200 mm \times 200 mm) was firstly cut into six rectangles of equal size, and then the paper-cell screen was placed on the paper with close contact (Step (1), Fig. 1) and the crayon was rubbed on the screen (Step (2), Fig. 1). To ensure enough solid wax printed on the paper, a smooth metal utensil was used to rub the screen (Step (3), Fig. 1). After the paper was wax-screen-printed, it was placed on the heating board together with the screen, and the wax was melted into

the paper to form the wax-patterned paper (Step (4), Fig. 1). Next, the electrode screen was placed on the patterned paper (Step (5), Fig. 1). Subsequently, the carbon ink was applied onto the electrode screen, and screen-printed onto the patterned paper to create the electrodes with the help of a squeegee (Steps (6) and (7), Fig. 1). Finally, the carbon electrodes-containing paper was separated from the electrode screen, and dried for about 5 h in air at ambient temperature instead of being cured in an oven (Step (8), Fig. 1). Following the fabrication of the paper-based device, both screens were treated to remove the residual wax or ink, which allowed the screens to be reused. These SP-ACE-EC- μ PADs can be fabricated in small bulk.

2.4 Preparation of the samples and enzyme solutions

Standard solutions of glucose or uric acid were prepared as follows: standard glucose solutions—20 \times PBS was diluted to 10 \times PBS using DI water and then glucose was dissolved in the diluted buffer at concentrations ranging from 0 to 10 mM; standard uric acid solutions—uric acid was dissolved in NaOH solution (50 mL, 50 mM) and then sonicated for approximately 5 min. The uric acid solution (0.01 M) was diluted with 5 \times PBS buffer to prepare standard solutions with concentrations from 0 to 2 mM.

Real urine samples that contained glucose or uric acid were prepared according to the following procedure: a real urine sample was obtained from an anonymous donor and then mixed with 20 \times PBS buffer in the same volume. As a result, the concentration of urine was diluted twice, and the obtained buffer had the same situation as that in the standard glucose solution. Next, the standard glucose solution was added into the urine sample, with increasing glucose concentrations of 0.25, 0.5 and 0.75 mM, respectively. Similarly, the concentrations of uric acid in urine were increased to be 0.1, 0.2 and 0.3 mM, respectively. A background signal was obtained by replacing the enzyme with an equivalent mass of BSA.

Two enzyme solutions were prepared with the following concentrations: (1) 280 U/mL glucose oxidase, 600 mM $K_3[Fe(CN)_6]$ and 1 M KCl in 1 \times PBS buffer; and (2) 14 U/mL uricase, 100 mM $K_3[Fe(CN)_6]$ and 1 M KCl in 1 \times PBS buffer.

2.5 EC assay using the SP-ACE-EC- μ PAD

The EC behavior of the SP-ACE-EC- μ PAD was characterized using cyclic voltammetry (CV) before detecting the analytes. Ferrocene carboxylic acid (2 mM) in KCl (0.5 M) was used as a model electroactive compound. Six different scan rates (50, 100, 200, 300, 400 and 500 mV/s) were applied to the working electrode (versus the carbon pseudo-reference electrode). The chronoamperometric assay for the determination of glucose or uric acid concentration in the standard or urine

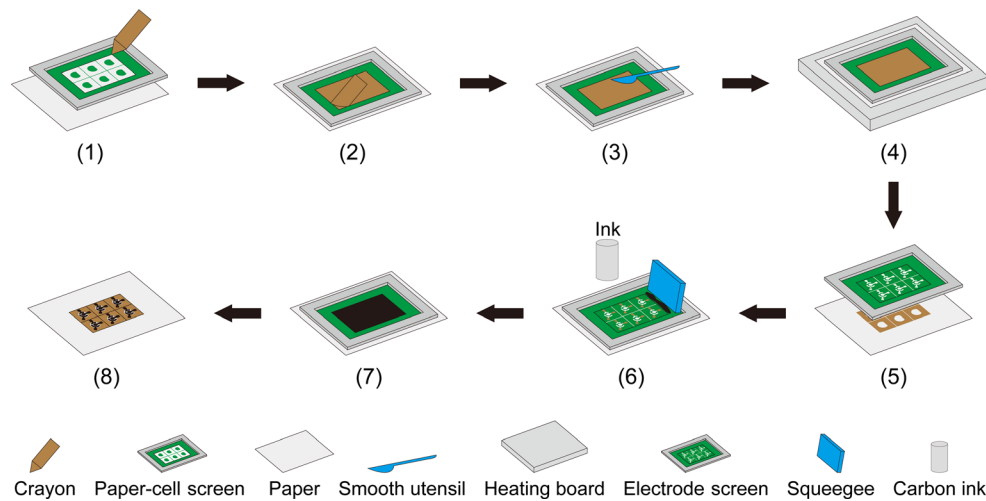


Fig. 1 Schematic of the fabrication process for SP-ACE-EC- μ PADs. (1) A paper-cell screen that can be rubbed with a crayon was placed on the paper. (2, 3) The screen was rubbed in turn with a crayon and a smooth utensil. (4) The printed paper was placed on the heating board together with the screen, and the wax was melted into the paper to the wax-

patterned paper. (5) The electrode screen was placed on the patterned paper. (6, 7) Carbon ink was screen-printed onto the paper. (8) The resulting paper was separated from the electrode screen, and dried in air at ambient temperature

samples involved spotting 2 μ L of enzyme solution onto the EC cell of the paper-based device. After drying in air for 20 min, the enzyme was uniformly absorbed in the paper. The solutions being analyzed (20 μ L) were then added to the paper-based device and allowed to react for 3 min. A step potential (300 mV) was applied to the working electrode (versus carbon pseudo-reference electrode), and the resulting current was monitored as a function of time. Each solution was dropped onto the opposite surface of the screen-printed paper, which allowed the solution to spread in the EC cell.

3 Results and discussion

3.1 Wax screen-printing of μ PADs

Wax screen-printing has been previously used for the fabrication of μ PADs (Dungchai et al. 2011; Wang et al. 2012, 2013). However, it has required high heating temperatures and long heating times for efficient penetration of the wax into the paper, which consumes large amounts of energy. Additionally, the wax on the screen in traditional wax screen-printing processes is not completely used for the formation of hydrophobic barriers in the paper. To overcome these shortcomings, we improved two key steps within the fabrication process of the wax screen-printing method: (1) once the screen was rubbed with a crayon, a smooth metal utensil was used to rub the screen to ensure more wax was transferred onto the paper substrate; and (2) both the paper and screen were placed on a heating board, instead of heating only the wax-screen-printed paper.

To evaluate the effectiveness of these improvements, μ PADs were fabricated using the traditional method for comparison (Fig. S1). Photos of each device were taken using a digital camera after the dye solution (20 μ L) was allowed to spread for 1 min in the wax-screen-printed μ PADs. The upper three rows of Fig. 2a show the traditional μ PADs after exposure to the dye solution using three different conditions (30 and 60 s melting time at 100 $^{\circ}$ C, as well as 30 s melting time at 75 $^{\circ}$ C). It was clear that the fabrication of the traditional μ PADs under these conditions was not successful with any of the screens that were used. Three possible reasons for this phenomenon are as follows: (1) similar to the previous work (Dungchai et al. 2011), the inadequate melting temperature and time might adversely affect the spreading and penetration of wax into paper; (2) the mere rubbing of the crayon against the screen might not cause enough wax to be printed on the paper surface; and (3) in the case of the separation of the paper from the screen, the wax that remained in the mesh openings of the screen would not be melted into the paper. Conversely, our screen-printing process was successful with each screen for the construction of μ PADs at a relatively low heating temperature and short melting time (5 s at 75 $^{\circ}$ C), as seen in the bottom row of Fig. 2a. These photos showed that more wax had melted into the paper, which formed well-defined hydrophobic barriers that ensured that the dye solutions were confined to the hydrophilic cells. In this work, the use of a smooth metal utensil ensured more wax was screen-printed on the paper surface. Additionally, when the paper-cell screen was heated together with the paper, the wax that remained in the mesh openings of the screen also melted into the paper. The weight of the screen ensured that the paper had efficient contact with the heating board.

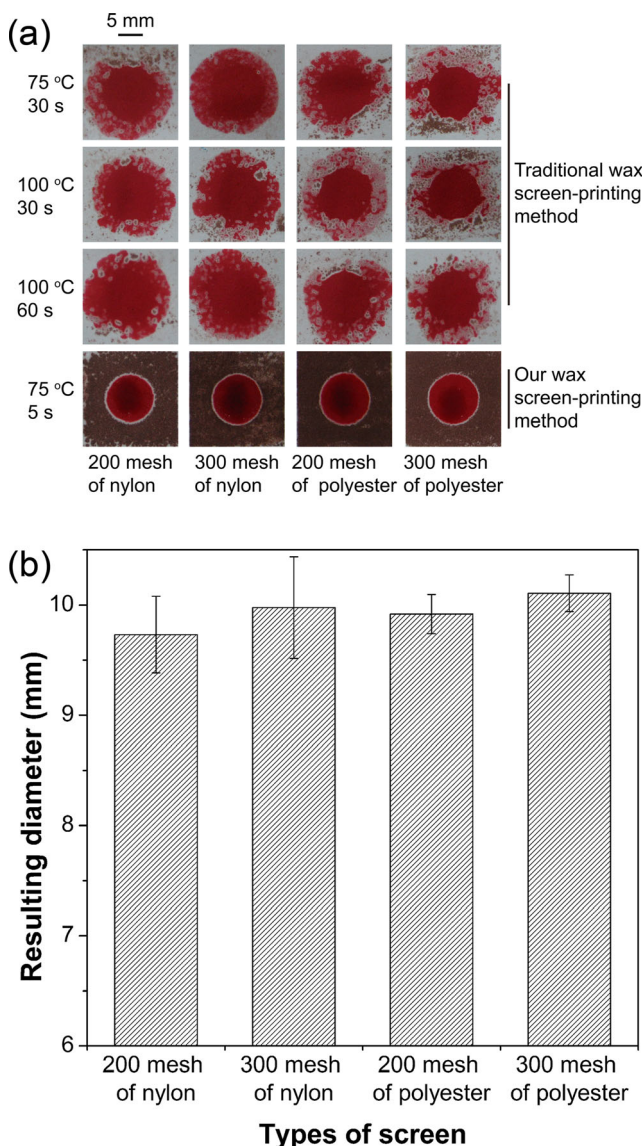


Fig. 2 **a** Comparison of μ PADs fabricated using two different wax screen-printing methods. Four different paper-cell screens were used, as shown below the panel. Three different combinations of heating temperature and time were chosen for the traditional fabrication method, while the heating condition of at 75 °C for 5 s could be used for the presented fabrication method, as labeled at the left of the panel. **b** Influence of the types of paper-cell screens on the resulting diameter of the paper-based cell wax-screen-printed by the presented fabrication method. Here, the paper-based cell was designed to be 11 mm in diameter, and 20 μ L of carmine dye solution was added into the cell to clearly reveal its contour. Error bars represent the standard deviations of five independent measurements

The μ PADs were fabricated stably when using each of the four different paper-cell screens (Fig. S2). However, the use of different screens resulted in differences in the average diameter of the paper-based cells (Fig. 2b). This may have been because the wax loading in these experiments was controlled by the thickness of the screen, the size of the mesh openings and the material that the screen matrix was made from. When the 300-mesh polyester screen was used, the resulting

diameter was the largest with the smallest standard error, which was closest to the target diameter. Additionally, the fabrication process when using the 300-mesh polyester screens was relatively stable. Conversely, the nylon screens resulted in relatively bad μ PADs.

3.2 Characterization of SP-ACE-EC- μ PADs

The carbon electrodes used in the SP-ACE-EC- μ PADs were investigated. These electrodes were simultaneously screen-printed using carbon ink on the hydrophilic and hydrophobic areas of the device, and the working area of the electrodes was on the hydrophilic portion of the device. The presented system is different from most other systems in which electrode materials, such as carbon, gold, and silver/silver chloride, are batch-fabricated onto a substrate (Carvalho et al. 2010; Dungchai et al. 2011). Ferrocene carboxylic acid was used as a model redox-active compound to characterize the electrode system, which has become commonplace for benchmarking paper-based EC devices (Main et al. 2013; Nie et al. 2010b).

CV can be used for quantitative analysis, and as a method to study the nature and mechanisms of electrode reactions, while giving the kinetic parameters of electrode processes. Characteristic CV voltammograms at different scan rates are shown in Fig. 3a. The voltammograms exhibited a reversible EC behavior. The polarization over-potential of the devices, which is defined as the difference between potentials at the cathodic peak current (i_{pc}) and the anodic peak current (i_{pa}), ranged from 60 to 89 mV. These values were close to the theoretical value of 59 mV for the ferrocene redox pair (Nie et al. 2010b). Additionally, the peak current ratio (i_{pc}/i_{pa}) was close to unity for all scan rates used. These results indicated that rapid electron transfer was occurring at the electrodes, with no side reactions. Next, the dependence of the peak current on the scan rate was examined (Fig. 3b). The cathodic and anodic peak currents were found to be linearly proportional to the square root of the scan rate between 50 and 500 mV/s (R^2 is 0.9919 and 0.9910, respectively). Additionally, there was no significant difference (<3 %) in the slopes of the forward and reverse sweeps. These results indicated that mass transfer within the SP-ACE-EC- μ PADs was a diffusion controlled process, similar to that of traditional EC cells. Here, it is necessary to note that similar to previous work (Määttä et al. 2013; Dungchai et al. 2009), potassium ferricyanide, as one of important EC mediators, could also be chosen as a model analyte for the CV experiments carried out with the proposed paper-based devices, and the obtained results were similar to those using ferrocene carboxylic acid (Fig. S3). Additionally, the CV experiments using silver/silver chloride as the reference electrode have been performed as the control. It has been shown in Fig. S4 that the polarization over-potential was from 58 to 70 mV, the peak current ratio (i_{pc}/i_{pa}) got close to 1.0,

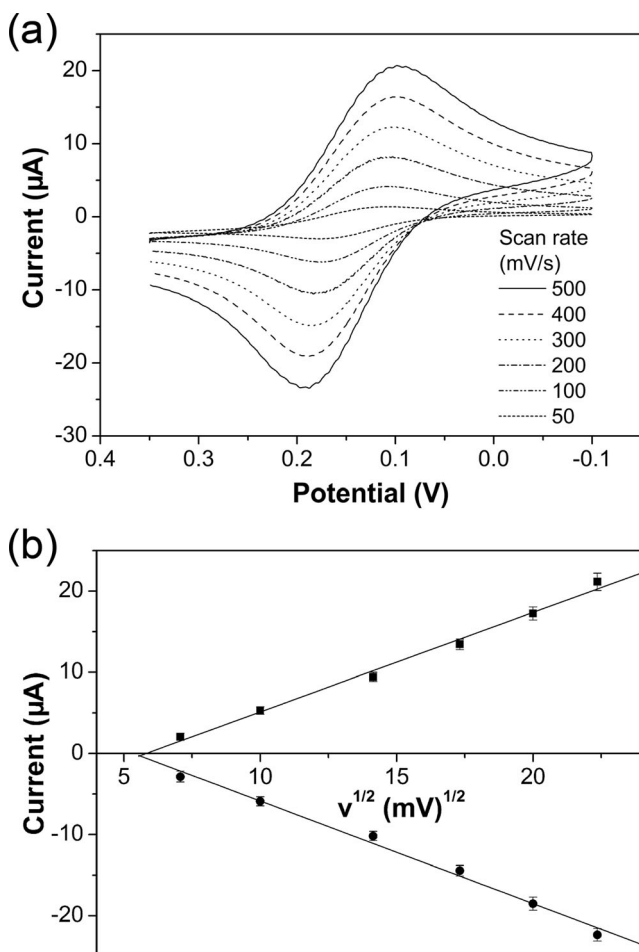


Fig. 3 Electrochemical characterization of the SP-ACE-EC- μ PADs. **a** Typical cyclic voltammograms of ferrocene carboxylic acid at different scan rates. **b** Plot of the peak current versus the square root of the scan rate ($v^{1/2}$). The fitted linear regression equations were $y = 1.2251x - 7.1269$ ($R^2 = 0.9919$, cathodic) and $y = -1.2630x + 6.7565$ ($R^2 = 0.9910$, anodic). Error bars represent the standard deviations of five independent measurements

and the cathodic and anodic peak currents were linearly proportional to the square root of the scan rate (50–500 mV/s) (R^2 is 0.9757 and 0.9740, respectively). These results showed that the CV characteristics obtained using carbon reference electrode was comparable to that using the silver/silver chloride reference electrode, similar to the case in a previous report (Nie et al. 2010b). Therefore, the proposed carbon-based three-electrode configuration can be favorably adopted for analytical application.

3.3 Analytical performance of the SP-ACE-EC- μ PADs

The analytical performance of the SP-ACE-EC- μ PADs was evaluated by assaying standard solutions of glucose (0–10 mM) or uric acid (0–2 mM). Urine usually contains from 0.1 to 0.8 mM glucose, with higher levels indicating health problems such as diabetes. Uric acid is an important nitrogen-

containing compound found in healthy human urine at concentrations from 0.2 to 4.4 mM. Abnormal levels are linked to a series of illnesses, including gout, Lesch–Nyhan syndrome and renal diseases (Kanyong et al. 2012). Chronoamperometry was chosen for the detection of glucose and uric acid because it is accurate, highly sensitive, and can be used with simple and portable EC readers. 2 μ L of enzyme solution was applied onto the paper-based cell, and then the device was dried in air to enable the enzyme to be uniformly absorbed in the paper. It has been found that the drying time of 20–60 min could result in a relatively strong EC signal (Fig. S5). Thus, 20 min was selected as the optimal drying time for subsequent experiments. The chronoamperometric curves for the measurement of standard glucose solutions are shown in Fig. 4a, while the insert shows the calibration curve in which the currents were recorded at 11 s. The calibration curve exhibited a linear response from 0

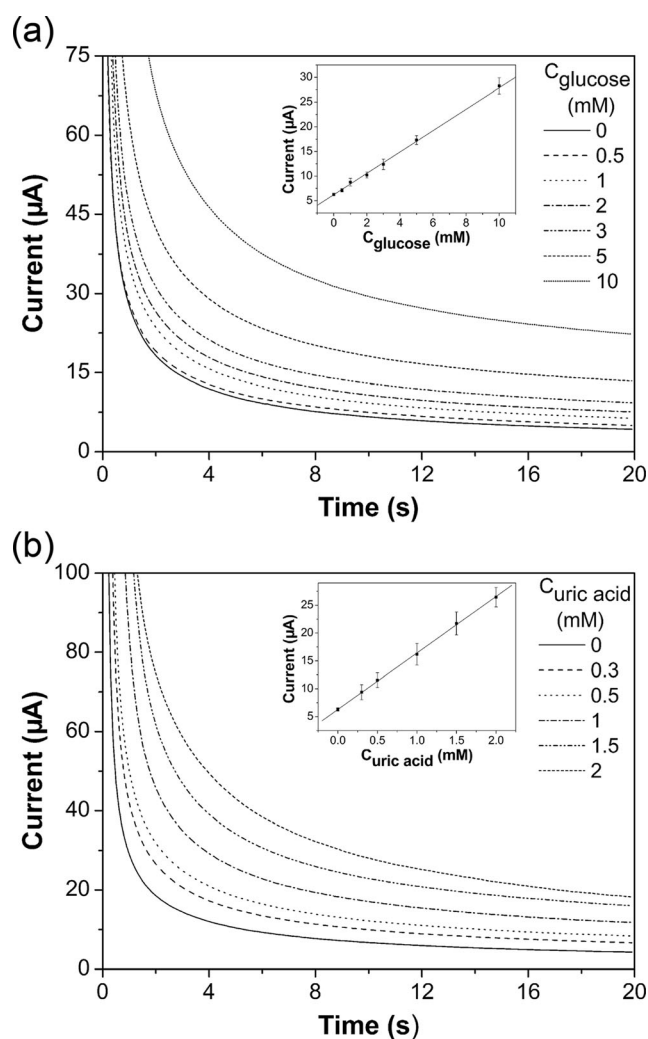


Fig. 4 Representative chronoamperometric curves for glucose (**a**) or uric acid (**b**) standard solutions. The calibration plots are shown in the insert, which were fitted to the linear regression equations $y = 2.2094x + 6.1161$ ($R^2 = 0.9987$) (glucose) and $y = 10.1363x + 6.2960$ ($R^2 = 0.9997$) (uric acid). Error bars represent the standard deviations of five independent measurements

to 10 mM, with a limit of detection (LOD) of 0.35 mM ($R^2 = 0.9987$, $n = 5$). The LOD was calculated to be the concentration that produced a signal three times the standard deviation of a blank. Similarly, a linear relationship was observed between the currents and the uric acid concentrations from 0 to 2 mM, with a LOD of 0.08 mM ($R^2 = 0.9997$, $n = 5$) (Fig. 4b). The relative standard deviations for all concentrations of glucose were between 1.9 and 8.8 %, and those for uric acid were between 4.5 and 14.4 %, which are acceptable values for reproducibility in these devices. In addition to that, the detection limits obtained on the proposed EC device are comparable to or lower than those in other paper-based EC devices where different fabrication methods and electrode materials were applied. On these previously-reported devices, the glucose assay could have a LOD of 0.18 mM (Lawrence et al. 2014), 0.22 mM (Nie et al. 2010b), 0.35 mM (Zhao et al. 2013) or 1.44 mM (Nie et al. 2010a), and the uric acid assay could have a LOD of 0.02 mM (Carvalho et al. 2010), 0.5 mM (WitkowskaNery et al. 2016), 0.52 mM (Zhao et al. 2013), 1.38 mM (Dungchai et al. 2009). Within the work by Kubota and co-workers, the LOD of 0.02 mM for uric acid may be attributed to that the separation and enrichment procedures were well integrated with the EC detection on the paper-based device (Carvalho et al. 2010). For the presented SP-ACE-EC- μ PAD, its analytical sensitivity can be improved by a series of inexpensive and straightforward means such as noble metal nanoparticles-based electrode modification to enhance the electroactivity of the screen-printed carbon electrode (Iwamoto et al. 2009), improved enzyme immobilization to enhance the activity of enzyme and the direct electron transfer between the enzyme's active sites and the electrode (Wang et al. 2009; Zhang et al. 2004), the mechanical grinding of the surfaces of carbon electrodes to strengthen the adsorption of analyte at the electrode surface (Hason et al. 2009), and the use of H_2O_2 transducer to improve analytical performances (Iveković et al. 2012).

3.4 Analysis of glucose and uric acid in real urine samples using the SP-ACE-EC- μ PADs

Artificial urine samples, rather than real urine samples, are often used for the detection of analytes of interest using paper-based EC devices. In this work, we were able to detect the levels of glucose and uric acid in real urine samples, which demonstrated the potential for real-world use of the SP-ACE-EC- μ PADs. Chronoamperometry, in combination with the standard addition method, was used for the determination of glucose or uric acid in real urine samples that were spiked with 0–0.75 mM glucose or 0–0.3 mM uric acid. The determination was performed on double-diluted urine samples (20 μ L) using fresh paper-based devices for each measurement. The results for the detection of glucose in real urine are shown in Fig. 5a (the insert shows the relationship between the chronoamperometric current response and the concentration of added glucose). The concentration of glucose in the diluted urine was determined to be 0.3387 mM.

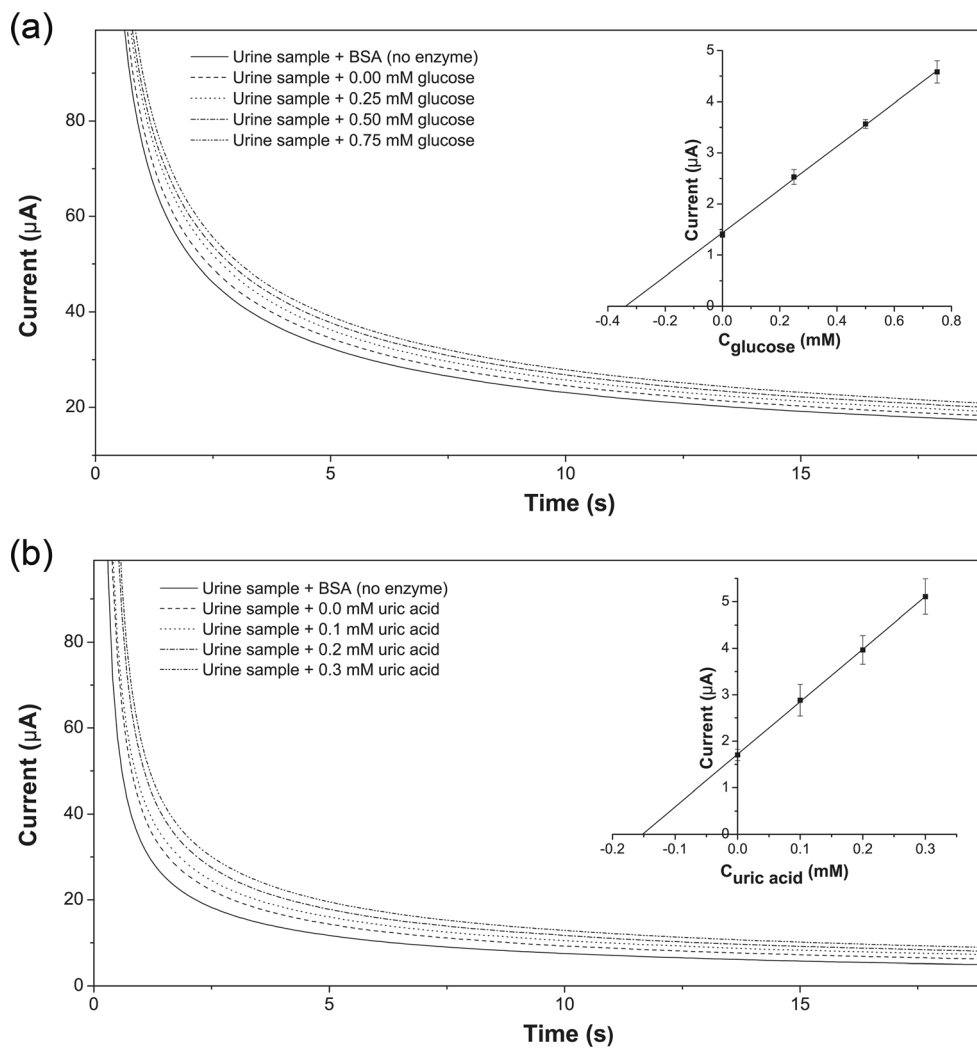
Thus, the glucose concentration in the real urine sample was approximately 0.68 mM, which was the same as the case of the anonymous donor. Similarly, the concentration of uric acid in the real urine sample was approximately 0.30 mM, as expected for the anonymous donor (Fig. 5b). Note that we first proposed the coupled chronoamperometry and standard addition method for paper-based microfluidic detection of glucose and uric acid in real urine samples. Additionally, the presented method has the potential to access urine samples from diabetic patients. As shown in Fig. S6, the concentrations of glucose and uric acid in the diabetic urine samples were determined to be 11.20 mM and 4.03 mM, respectively. It can be seen from Fig. 5 and Fig. S6 that the proposed paper-based EC device has the potential for the detection of target analytes within a wide concentration range.

3.5 Limitations and future work

Although the presented SP-ACE-EC- μ PAD can be prepared in a simple, inexpensive and energy-efficient way and applied for the detection of target analytes, it also has three main limitations. Firstly, relative to the wax screen-printing of paper-based cells, the screen-printing of carbon electrodes on wax-patterned papers requires a long time (~ 5 h) for drying of the electrodes in air at ambient temperature. But, it should be noted that such a drying way has several advantages such as simplicity of the process, no need of additional electric heating equipment (e.g. oven), energy-saving and environment-friendly. Secondly, the working electrode of the SP-ACE-EC- μ PAD is a bare carbon screen-printed electrode, without any nanomaterial-based electrode modification, and as a result its applications may be limited. Thirdly, the presented paper-based EC device also has only used with an indispensable expensive potentiostat instrument, which may limit its applications in low-resource settings.

To circumvent these limitations, further work will focus on the following three aspects. Firstly, two screen-printing processes are optimized to reduce the time needed for the fabrication of the paper-based device. Similar to our recent work (Chen et al. 2016), carbon ink-screen-printing can be used to fabricate the electrodes onto the paper, and then the wax is applied to form the hydrophobic barrier on the electrode-patterned paper. Such a fabrication procedure can allow the baking of electrodes at relatively high temperatures, and thus the preparation of the paper-based device can be accomplished in a few minutes. Secondly, appropriate surface modification strategies such as layer-by-layer assembly (Ariga et al. 2014) and self-assembled monolayer (Cheng et al. 2014) are used for decoration and modification of the present device. It should be noted that the compatibility of some surface modification strategies with the paper-based devices has been well-established (Wang et al. 2014; Kong et al. 2014; Määttä et al. 2013; Liu and Crooks 2012; Xiang and Lu 2011). Thirdly, the device may be tested for compatibility with a new or existing low-cost potentiostatic control strategy.

Fig. 5 Chronoamperograms from the analysis of real urine samples with BSA (no enzyme), and of real urine samples with added glucose (0, 0.25, 0.50, and 0.75 mM) (a) or uric acid (0, 0.1, 0.2, 0.3 mM) (b). The calibration plots of the chronoamperometric current response versus the concentration of added glucose or uric acid are shown in the insert, with the fitted linear regression equations $y = 4.2317x + 1.4333$ ($R^2 = 0.9994$) (glucose) and $y = 11.2968x + 1.7202$ ($R^2 = 0.9998$) (uric acid), respectively. A background signal with no enzyme was subtracted from the sensing signals to obtain the insert plot. Error bars represent the standard deviations of five independent measurements



For example, a mobile phone (Delaney et al. 2013) or personal glucose meter (Xiang and Lu 2011) has the potential to be used for the inexpensive potentiostatic control. Ideally, the SP-ACE-EC- μ PAD should be integrated with paper-based electronic elements (such as paper-based battery (Wang et al. 2014; Liu and Crooks 2012)) to construct a more fully integrated EC device, without the need of peripheral electrical equipment.

4 Conclusions

In this work, we have fabricated novel paper-based devices that were wax-screen-printed and incorporated screen-printed carbon electrodes. These devices allowed the EC detection of both glucose and uric acid in real urine samples. The use of inexpensive carbon ink, wax and paper, in combination with simple screen-printing technology allowed the fabrication of low-cost and simple EC devices for the detection of analytes of interest. We optimized the wax-screen-printing approach, which led to the use of

a lower heating temperature and a shorter heating time. The carbon electrodes that were screen-printed on patterned paper exhibited a good EC response towards ferrocene carboxylic acid, with a reversible reaction process and diffusion-controlled mass transfer. The detection of glucose and uric acid in standard solutions exhibited an acceptable linear range, detection limit and reproducibility. Significantly, the SP-ACE-EC- μ PADs were able to detect glucose and uric acid in real-world urine samples. We have shown that the proposed fabrication method and the resulting EC devices have great promise for clinical diagnosis, food detection and environmental monitoring.

Acknowledgments This research is supported by the National Natural Science Foundation of China (No. 81571765), Guangzhou Science and Technology Program (No. 2014J4100030), and Guangdong Science and Technology Program (No. 2014A020212503; No. 2016A020215143). We thank Dr. Bin Wu at Guangzhou First People's Hospital for his help in collecting the urine samples.

References

- K. Ariga, Y. Yamauchi, G. Rydzek, Q.M. Ji, Y. Yonamine, K.C.W. Wu, J.P. Hill, *Chem. Lett.* **43**, 36–68 (2014)
- R.F. Carvalho, M.S. Kfoury, M.H.D. Piazzetta, A.L. Gobbi, L.T. Kubota, *Anal. Chem.* **82**, 1162–1165 (2010)
- L. Chen, C.S. Zhang, D. Xing, *Sens. Actuators B* **237**, 308–317 (2016)
- X.Y. Cheng, S.B. Lowe, P.J. Reece, J.J. Gooding, *Chem. Soc. Rev.* **43**, 2680–2700 (2014)
- J.L. Delaney, C.F. Hogan, J. Tian, W. Shen, *Anal. Chem.* **83**, 1300–1306 (2011)
- J.L. Delaney, E.H. Doeven, A.J. Harsant, C.F. Hogan, *Anal. Chim. Acta* **790**, 56–60 (2013)
- N. Dossi, R. Toniolo, E. Piccin, S. Susmel, A. Pizzariello, G. Bontempelli, *Electroanalysis* **25**, 2515–2522 (2013)
- W. Dungchai, O. Chailapakul, C.S. Henry, *Anal. Chem.* **81**, 5821–5826 (2009)
- W. Dungchai, O. Chailapakul, C.S. Henry, *Analyst* **136**, 77–82 (2011)
- S. Hasoň, V. Vetterl, F. Jelen, M. Fojta, *Electrochim. Acta* **54**, 1864–1873 (2009)
- D. Iveković, M. Japac, M. Solar, N. Živković, *Int. J. Electrochem. Sci.* **7**, 3252–3264 (2012)
- M. Iwamoto, S. Tokonami, H. Shiigi, T. Nagaoka, *Res. Chem. Intermed.* **35**, 919–930 (2009)
- L. Jiang, M. Mancuso, Z. Lu, G. Akar, E. Cesarman, D. Erickson, *Sci. Rep.* **4**, 4137 (2014)
- P. Kanyong, R.M. Pemberton, S.K. Jackson, J.P. Hart, *Anal. Biochem.* **428**, 39–43 (2012)
- F.Y. Kong, S.X. Gu, W.W. Li, T.T. Chen, Q. Xu, W. Wang, *Biosens. Bioelectron.* **56**, 77–82 (2014)
- C.S.K. Lawrence, S.N. Tan, C.Z. Floresca, *Sens. Actuators B* **193**, 536–541 (2014)
- H. Liu, R.M. Crooks, *Anal. Chem.* **84**, 2528–2532 (2012)
- M. Liu, C.S. Zhang, F.F. Liu, *Anal. Chim. Acta* **891**, 234–246 (2015)
- Y. Lu, W.W. Shi, L. Jiang, J.H. Qin, B.C. Lin, *Electrophoresis* **30**, 1497–1500 (2009)
- A. Määttä, D. Fors, S. Wang, D. Valtakari, P. Ihalainen, J. Peltonen, *Sens. Actuators B* **160**, 1404–1412 (2011)
- A. Määttä, U. Vanamo, P. Ihalainen, P. Pulkkinen, H. Tenhu, J. Bobacka, J. Peltonen, *Sens. Actuators B* **177**, 153–162 (2013)
- A. Määttä, A. Fallarero, J. Kujala, P. Ihalainen, P. Vuorela, J. Peltonen, *AMB Express* **4**, 32 (2014)
- V. Main, K. Kadimisetty, S. Malla, A.A. Joshi, J.F. Rusling, *Environ. Sci. Technol.* **47**, 1937–1944 (2013)
- A.W. Martinez, S.T. Phillips, M.J. Butte, G.M. Whitesides, *Angew. Chem. Int. Ed.* **46**, 1318–1320 (2007)
- A.W. Martinez, S.T. Phillips, G.M. Whitesides, *Anal. Chem.* **82**, 3–10 (2010)
- Z. Nie, F. Deiss, X. Liu, O. Akbulut, G.M. Whitesides, *Lab Chip* **10**, 3163–3169 (2010a)
- Z. Nie, C.A. Nijhuis, J. Gong, X. Chen, A. Kumachev, A.W. Martinez, M. Narovlyansky, G.M. Whitesides, *Lab Chip* **10**, 477–483 (2010b)
- J. Noiphung, T. Songjaroen, W. Dungchai, C.S. Henry, O. Chailapakul, W. Laiwattanapaisal, *Anal. Chim. Acta* **788**, 39–45 (2013)
- T. Nurak, N. Praphairaksit, O. Chailapakul, *Talanta* **114**, 291–296 (2013)
- P. Rattanasat, W. Dungchai, D. Cate, J. Volckens, O. Chailapakul, C.S. Henry, *Anal. Chem.* **86**, 3555–3562 (2014)
- M. Santhiago, L.T. Kubota, *Sens. Actuators B* **177**, 224–230 (2013)
- L.Y. Shiroma, M. Santhiago, A.L. Gobbi, L.T. Kubota, *Anal. Chim. Acta* **725**, 44–50 (2012)
- T. Songjaroen, W. Dungchai, O. Chailapakul, W. Laiwattanapaisal, *Talanta* **85**, 2587–2593 (2011)
- S.N. Tan, L. Ge, W. Wang, *Anal. Chem.* **82**, 8844–8847 (2010)
- S.N. Tan, L. Ge, H.Y. Tan, W.K. Loke, J. Gao, W. Wang, *Anal. Chem.* **84**, 10071–10076 (2012)
- N.K. Thom, G.G. Lewis, K. Yeung, S.T. Phillips, *RSC Adv.* **4**, 1334–1340 (2014)
- Y.T. Wang, L. Yu, Z.Q. Zhu, J. Zhang, J.Z. Zhu, C.H. Fan, *Sens. Actuators B* **136**, 332–337 (2009)
- S.M. Wang, L. Ge, X.R. Song, J.H. Yu, S.G. Ge, J.D. Huang, F. Zeng, *Biosens. Bioelectron.* **31**, 212–218 (2012)
- Y.H. Wang, S.M. Wang, S.G. Ge, S.W. Wang, M. Yan, D.J. Zang, J.H. Yu, *Anal. Methods* **5**, 1328–1336 (2013)
- Y.H. Wang, L. Ge, P.P. Wang, M. Yan, J.H. Yu, S.G. Ge, *Chem. Commun.* **50**, 1947–1949 (2014)
- E. WitkowskaNery, M. Santhiago, L.T. Kubota, *Electroanalysis* **28**, 2245–2252 (2016)
- Y. Xiang, Y. Lu, *Nat. Chem.* **3**, 697–703 (2011)
- A.K. Yetisen, M.S. Akram, C.R. Lowe, *Lab Chip* **13**, 2210–2251 (2013)
- F.F. Zhang, X.L. Wang, S.Y. Ai, Z.D. Sun, Q. Wan, Z.Q. Zhu, Y.Z. Xian, L.T. Jin, K. Yamamoto, *Anal. Chim. Acta* **519**, 155–160 (2004)
- C.S. Zhang, D. Xing, Y.Y. Li, *Biotechnol. Adv.* **25**, 483–514 (2007)
- C. Zhao, M.M. Thuo, X.Y. Liu, *Sci. Technol. Adv. Mater.* **14**, 054402 (2013)